

# The relationship between the 5-min oscillation and 3-min oscillations at the umbral/penumbral sunspot boundary

Xinping Zhou<sup>1</sup> · Hongfei Liang<sup>1</sup>

Received: 16 November 2015 / Accepted: 21 December 2016 / Published online: 8 February 2017  
© Springer Science+Business Media Dordrecht 2017

**Abstract** Observations of the main sunspot of AR 11692 were carried out with the 1 m New Vacuum Solar Telescope (NVST) located on the Fuxian Solar Observatory (FSO) in  $H\alpha$  on March 13, 2013. The high cadence (up to 12 s)  $H\alpha$  intensity images help us to investigate the relationship between the 5-min oscillation and 3-min oscillation. It is found that running waves, periodically formed at the wave sources within umbra, propagate outward with the shape of partial arcs. The running waves run across the umbra–penumbra boundary and eventually disappear at the edge of penumbra. But there are obvious differences when we measure the period of running waves in different regions of a sunspot. The period is about 150 s when the running waves are located in umbra, which is a typical 3-min oscillation, and the period is about 300 s when the running waves are located in the penumbra, which is a typical 5-min oscillation. On the basis of time-slice images, we conclude that the waves form in the umbral region with the 5-min oscillation period, which can cause the brightness periodicity change in the umbra region with the 3-min period (in fact, is half of 5-min oscillation) and 5-min in the penumbra.

**Keywords** Sunspots · Oscillations

## 1 Introduction

Since the discovery of umbral flash in CaII H&K lines by Beckers and Tallant (1969), the oscillation phenomena has always been an important research project. Three years later,

umbra oscillations and running penumbra waves were revealed by different spectra lines (Beckers and Schultz 1972; Giovanelli 1972; Bhatnagar et al. 1972; Zirin and Stein 1972; Giovanelli 1972). In addition to sunspot oscillation, wave or oscillation phenomena have been observed everywhere in the solar atmosphere, for example, the largescale EUV wave (e.g., Shen and Liu 2012a, 2012b; Shen et al. 2013a), the filament oscillation (e.g., Shen et al. 2014a, 2014b, 2015), and the quasi-periodic fast magnetosonic waves (e.g., Shen and Liu 2012c; Shen et al. 2013b). These studies indicate that oscillations are a common phenomenon in the solar atmosphere with different heights. Alissandrakis et al. (1992, 1998) found that running waves, starting out as full circles around oscillating umbral element with a size of  $2 \sim 3''$ , propagated through whole active regions, including umbra and penumbra, with a regular fibril structure. Based on these results, they inferred that sunspot oscillations and running penumbra waves are probably manifestations of the same phenomenon of one kind of wave within solar active regions. Tsiropoula et al. (1996a, 1996b) also found waves in the outer 0.3 of the umbral radius that propagated through the inner part of the penumbra in active regions with regular fibril structure and propagating velocities of  $13\text{--}24 \text{ km s}^{-1}$ . Alissandrakis et al. (1999) and Tsiropoula et al. (2000) provided more clear evidence that these waves originated from oscillation elements inside the umbra and propagated through the penumbra.

Combining the observations carried out with three different telescopes, the Swedish Vacuum Solar Telescope, the Dutch Open Telescope, and the Swedish 1 m Solar Telescope at the Roque de los Muchachos Observatory on La Palma, Rouppe van der Voort et al. (2003) revealed that umbral flashes and running penumbral waves, combining upward shock propagation with coherent wave spreading over the entire spot, are closely related oscillatory phenomena.

✉ H. Liang  
lhf@ynao.ac.cn

<sup>1</sup> Department of Physics, Yunnan Normal University, 650500, Kunming, China

Kobanov and Makarchik (2004) found that the running umbral waves with a period of 2.8 min propagate outward from the sunspot center in the chromosphere. The phase velocity of the running umbral waves is  $45\text{--}60\text{ km s}^{-1}$  and their line-of-sight velocity amplitude is about  $2\text{ km s}^{-1}$ . Tziotziou et al. (2006) found that some running waves related to a shock smoothly propagated with an average speed of  $19\text{ km s}^{-1}$  from the umbra to penumbra through the umbra–penumbra boundary. An interesting phenomenon in their research is that the frequency of the waves decreased when the waves propagated from umbra to penumbra. By analyzing the data obtained by the Interferometric Bidimensional Spectropolarimeter (IBIS/DST), Löhner-Böttcher and Bello González (2015) also found signatures of running penumbral waves in photospheric layers. This result further supports the scenario of running penumbral waves being upward-propagating slow-mode waves guided by the magnetic field lines.

In this paper, we try to investigate the relationship between the 3-min umbra oscillation and 5-min penumbra oscillation in the sunspot. On March 13, 2013, observation of the main sunspot of AR 11692 with high temporal and spatial resolution were carried out with NVST by using the  $H\alpha$  line. Combining the methods of the time-slice image and wavelet analysis, we find that the running waves forming within umbra propagate outward continuously. When the running waves propagate from the umbra to the penumbra, their period changes from 297 to 153 s.

## 2 Observations

On March 13, 2013, the main sunspot of AR11692, located at N07 E38, was observed by the telescope NVST located in FSO with the  $H\alpha$  line. From 05:08:46UT to 05:47:55UT, 190 filtergrams were obtained under good seeing conditions for most of the time. The data were obtained with a  $1024'' \times 1024''$  CCD camera and the pixel size of the images was  $0.15''$ . The time intervals between images were 12 s. As show in Fig. 1 (left), the field of view that we used for analysis was  $265 \times 265$  pixels, containing the whole umbra and penumbra of the sunspot. It is well known that some distortions occur in the images due to the influences of the seeing-induced crosstalk, alignment error of the prisms, etc., during the observation. To correct the distortions and to ensure the possibility of the direct comparison between pixels in different images to the time series, a two-dimensional cross-correlation technique is employed to take care of the alignment of the images of our sequence. Furthermore, a subtraction image processing technique (Christopoulou et al. 2000) is employed to help us remove the sharp intensity gradient between the penumbra and the umbra, and the time varying phenomenon existing in the intensity images is enhanced.

In the intensity images, the intensity produced by the running waves is much less than the steady solar radiation intensity. To make the running waves much more noticeable, running difference images were used to enhance the image-varying phenomena. During the observations, the time resolution was up to 12 s per frame and the running waves propagated relatively slowly within the penumbra. To enhance the image-varying phenomena related to the running waves, we applied running difference images with a time interval of three frames (hereafter RDI3),  $\text{RDI3} = \text{image}_{i+3} - \text{image}_i$ , to highlight oscillation in the sunspot, where  $\text{image}_{i+3}$  and  $\text{image}_i$  are the  $i$ th and  $(i + 3)$ th intensity images (Liang et al. 2012). As shown in Fig. 1 (middle), we can see that the wavefronts in processed image could be better identified. The running waves have azimuthal extent as large as  $120^\circ$ , and propagate through the whole sunspot, including umbra and penumbra. In Fig. 1 (middle), there were four running waves originating from wave source A, one just formed at the wave source A, the second and third located near the boundary of umbra–penumbra and propagating outward, the fourth situated at the inner penumbra. They are forming partial arcs around its source A and most of them have clear tracks along the west direction. To facilitate the following analysis, we trace the waves along the black vertical dotted line. In the intensity images, the umbra is much darker related to the quiet region. In order to make the waves much more noticeable without introducing artifacts for the convenience of the latter analysis of the period, we take every pixel value by subtracting from each image the corresponding local average:  $I(x, y, N_i) = I(x, y, N_i) - \sum_i^N \frac{I(x, y, n_i)}{N}$ , where  $I(x, y, N_i)$  is the intensity of the light at the  $(x, y)$ th position of the  $i$ th image,  $N$  is the total number of selected images. We called this total image “Subtracting local total mean intensity” (hereafter SLTMI) image as shown in Fig. 1 (right). In the picture we can see that there is too much black or too much bright region, which can facilitate us to analyze the trace of the running waves. The equally spaced white crossings (A–J) in Fig. 1 were the sample points used to analyze the oscillation frequency.

Through the study of the three images in Fig. 1, we get that the contrast of umbra and penumbra of left image is big but it can clearly display the original appearance, RDI3 image is good at enhancing the contrast and showing the propagation process of the running waves; obviously, the contrast of SLTMI image is smaller than that of the original image and it is harder to see the running waves in this image, since we removed the sharp intensity contrast and every pixel was multiplied by the mean of the total pixel value at its local position, so without introducing the artifacts and convenience to research the real oscillation in sample points.

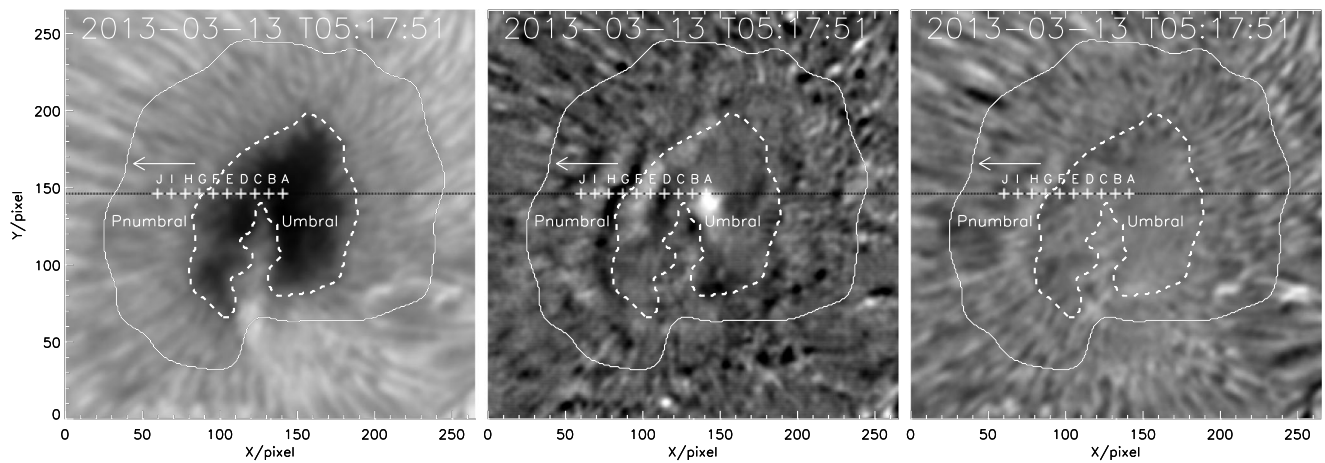


**Fig. 1** Sketch map of wave source within a sunspot. (Left) A sample intensity map of the sunspot in the  $H\alpha$  line. (Middle) A sample RDI3 image in the  $H\alpha$  line showing the running waves. (Right) A sample of the SLTMI image. The black horizontal dotted line is the position used to produce a spatiotemporal time slice image in Fig. 3. The white

crosses A–J mark the positions of the sample within the sunspot. The intensity profiles at sample points A–J, which are shown in Fig. 4, were used to analyze the oscillation period. The dotted white contour shows the  $H\alpha$  umbra–penumbra boundary, the solid white contour shows the approximate outer penumbra boundary

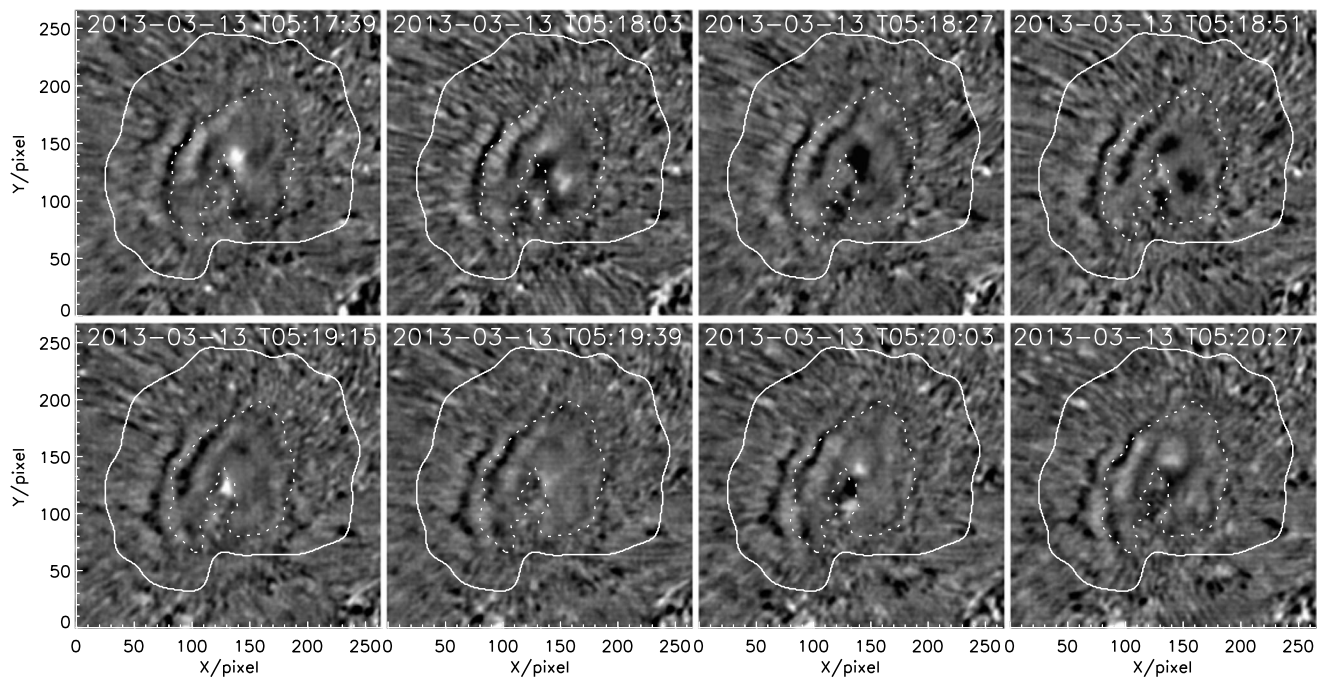


**Fig. 2** The evolution of running waves propagating from source A. The wave source is located in the center of each image with a field-of-view of  $265'' \times 265''$  pixels

### 3 Data analysis and results

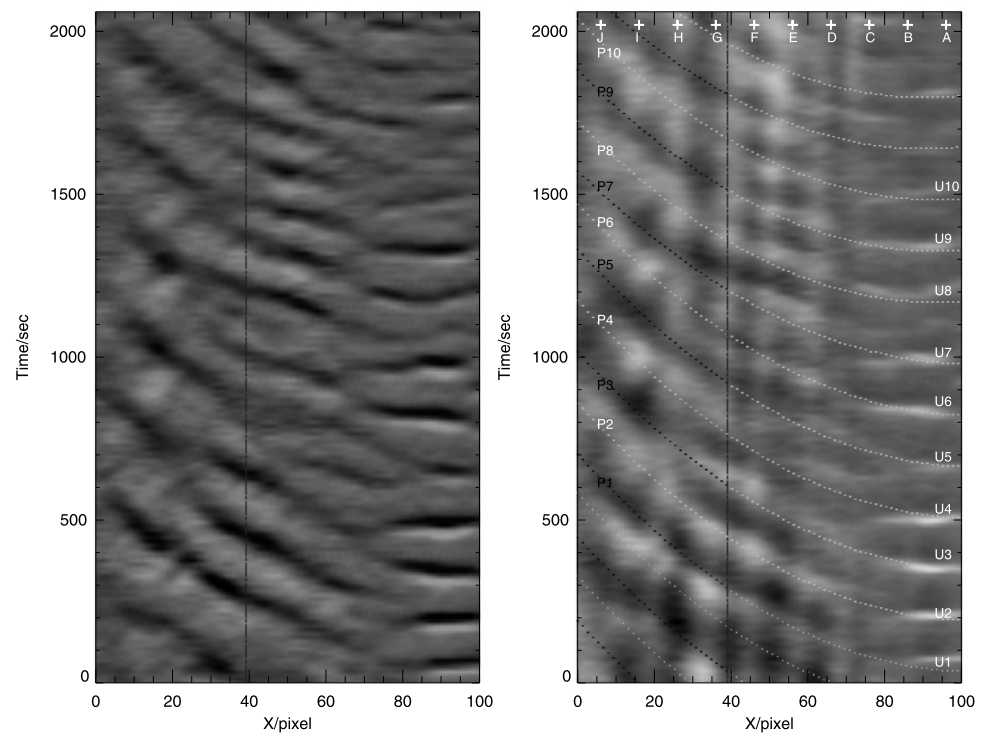
#### 3.1 Propagation path of running waves

To accurately investigate the association between 3-min and 5-min oscillations, 185 RDI3s were selected to create a movie which vividly demonstrates many aspects of the running waves. The movie shows that bright regions tend to reappear periodically at almost the same location, wave

source A. As shown in Fig. 2, running waves formed at source A have clear tracks with a time cadence of 24 s. The dotted white contour shows the  $H\alpha$  umbra–penumbra boundary while the solid white contour shows the approximate outer penumbra boundary. There are three running waves that propagate outwards and have an arc structure. One is shown to arrive at the penumbra; the second is on the umbra–penumbra boundary; and the third is formed just



**Fig. 3** Time-slice images along the *black horizontal dotted line* shown in Fig. 1. (*Left*) Applying the RDI3 image (Fig. 1, *middle*) makes the time-slice image. (*Right*) Using the SLTMI image in Fig. 1 (*right*) makes the time-slice image. The *vertical dotted line* indicates the approximate umbra–penumbra boundary. *Dotted quadratic curves* denote the tracks of running waves originating from wave source A, the *white crosses* (A–J) correspond to crosses (A–J) in Fig. 1. U1–U10 represent the wave crests of the sample point A, P1–P10 represent the wave troughs and wave crests of the sample point J



at the position of wave source A. With the evolution of the sunspot, the running waves propagate to the outer edge of penumbra, and at the RDI3 (05:19:15) another running wave is forming at the source A. As seen in Fig. 2, running waves propagate through the whole sunspot, including umbra and penumbra, and their evolution is smooth and continuous, propagating from source A.

The running difference images show that running waves are visible as propagating arcs in both umbra and penumbra, while in the penumbra they seem to have an azimuthal extent of  $120^\circ$  on the west side of the sunspot as shown in Fig. 2. To show the relationship between the 3-min and 5-min oscillations, we present time-slice images in Fig. 3 (left): they were created by applying the running difference data to enhance the process of the running wave propagating from the wave source A, which gives the velocity as a function of time along the horizontal black dotted line as shown in Fig. 1, starting from the position of approximately source A and propagating towards the penumbra. In Fig. 3 (right), we can clearly see the running wave propagating from the umbra to penumbra. There are 17 main strips which show the track of the running waves originating from wave source A in the time-slice image. These dark strips can almost be fitted into series of similar quadratic curves, denoted by the dotted curves in Fig. 3. These quadratic curves show that the velocity of the running waves decreases progressively along with the waves propagating from the wave source A to the outer penumbra. The dark and bright bands

show that there is a clear continuous wave originating from the source A (right part of the panel) propagating through the whole sunspot, including umbra and penumbra, which points out that the running waves within both umbra and penumbra have common origin. That is to say, most of the running waves in the penumbra can be traced back inside the umbra and seem to be a continuation of umbra waves. By analyzing the data obtained by New Solar Telescope at the Big Bear Solar Observatory, Su et al. (2016) discovered that the wavefronts form one-armed spiral structure. Once the spiral arms run across the umbra–penumbra boundary, they become running penumbral waves and propagate outwards continuously. These phenomena have been used to support the opinion that the umbral and penumbral waves propagate along the same inclined field lines.

Carefully observing the dotted curves from right to left in Fig. 3 (right), we find that the wave crest of running waves in the umbra transforms to trough or crest when it gets through the umbra–penumbra boundary and continues to propagate to the outer penumbra (U1–U10 are wave crests, and P1–P10 are alternating crests and troughs). We can judge that the frequency of the oscillation in the umbra is twice that of the penumbra. During the observation, the running waves, periodically formed at the wave source A, propagated outwards within the whole sunspot. The running waves produced periodical variation in light intensity within the sunspot, such as the sample points A–J.

### 3.2 Frequency behavior of the sample points

In Fig. 4, we used 150 image sections to plot the H velocity variations using the right image of Fig. 3 at sample points A–J, marked in Fig. 1. Time zero approximately corresponds to the dotted curves' (marked by U1 or P1) position, whose velocity variability is shown in the right panel of Fig. 3. The solid lines in Fig. 4 show time profiles of the  $H\alpha$  intensity at the sample points (A–J) in Fig. 1, which illustrates the umbra and penumbra intensity variation mainly derived from the running waves originating from wave source A. The marked sample A–E shows velocity variations for positions within the inner umbra, the marked sample F–G shows velocity of variations at the position just near the umbra–penumbra boundary, the marked sample H–J corresponds to the velocity variations for positions within the penumbra.

In order to accurately measure the oscillation periods of the running waves, we adopt the wavelet analysis method, an effective technique for extracting the period information from the signal within a time series, which has been developed in recent decades. The wavelet analysis method develops the idea of localized short-time Fourier transform and overcomes the shortcomings of short-time Fourier transform in single resolution and has the characteristics of multi-resolution analysis. Figure 5 shows the wavelet analysis results of the intensity variation curves of the sample points A–J. The result is used to support our statistical research of sunspot oscillation in the paper of Zhou et al. (2017). In the analysis, the function “Morlet” is taken as the basis function and a red-noise significance test is performed. In Fig. 5, the frequencies of the sample points A–J are determined by the global power, where the significance is above 95 %. It is found that the frequencies of sample points A–J are 6.7, 6.1, 6.7, 6.7, 6.7, 5.1, 5.0, 3.3, 3.5, and 3.3 mHz, respectively. These measured results show that there is an obvious difference between the frequency of the running waves within the umbra and penumbra. The frequency of the running waves within umbra is about twice that of the within penumbra. Similar results have been reported by Bogdan and Judge (2006) and Tziotziou et al. (2006). We also can notice an interesting trend that the peak values are scattered, but the valley values are close to the vicinity (average valley) value. But when looking at the sample position in the penumbra region (H–J), the velocity variations show a gradual increase from negative to positive values followed by a slow decrease back to negative values, and the wave crest and valley is symmetrical. The velocity variation (F–G) near the umbra–penumbra boundary has a similar shape to the sample position in the umbra. Our figures (especially Fig. 4) clearly show that the frequency of the umbral oscillation is about twice that of the penumbral oscillation. Furthermore, there is no smooth transition from one to the other near the

umbra–penumbra boundary. This has also been noticed by Christopoulou et al. (2001). Along the sample points A–J from the umbra to the penumbra, the average frequency in the umbra, umbra–penumbra boundary, and penumbra are: 6.55, 5.05, and 3.37 mHz, respectively, and the corresponding average periods are 153, 198, and 297 s. The results clearly indicate that the period of the running waves changes markedly at the umbra–penumbra boundary. The period of running waves within umbra is about one half of that of the running wave within penumbra. In the former analysis, the time-slice images show that the running waves continuously propagate through the whole sunspot. As for these running waves with completely different periods, we will try to find a reasonable explanation for these results in the following.

### 4 Discussions and summary

Investigating the periodic phenomenon within sunspots, such as umbral and penumbral oscillations, is an important method to detect their nature, physical mechanism, and the energy transport in the solar atmosphere. Although the research of solar oscillation has made great progress in recent decades, there are many issues related to these oscillation phenomena, such as their driving mechanism and the frequency reducing sharply at the umbra–penumbra boundary, that wait for further research. By analyzing the observations of AR11692 collected on March 13th 2013, we find that the running waves, originated from oscillating elements within the umbra, propagate outwards with decreasing radial speed. The running waves run across the umbra–penumbra boundary and propagate within the penumbra. These phenomena show that the running penumbra waves are the continuation of the running umbra waves. Analysis of time-slice images also shows that the waves in the penumbra can be traced inside the umbra: the wave crests transformed to wave troughs continue propagating in the penumbral region. Although we cannot provide the detailed physical progress for the observed period changes, our findings imply that the umbral and penumbral oscillations belong to the same running wave system and they are probably produced by the same physical mechanism. The reasons for the frequency change could be the physical conditions of the solar atmosphere, such as plasma density and inclination of the magnetic field.

By using the wavelet analysis method to analyze the  $H\alpha$  intensity profiles at 10 sample points within the sunspot, we obtain the periods of running waves within the umbra and penumbra, which are about 150 and 300 s, respectively. Evans and Roberts (1990) associated the running waves to the fast magneto-acoustic waves and suggested that the running waves may originate from near the center of the umbra. Furthermore, there is significant progress in the theory to incorporate the nature of 3-min umbra and

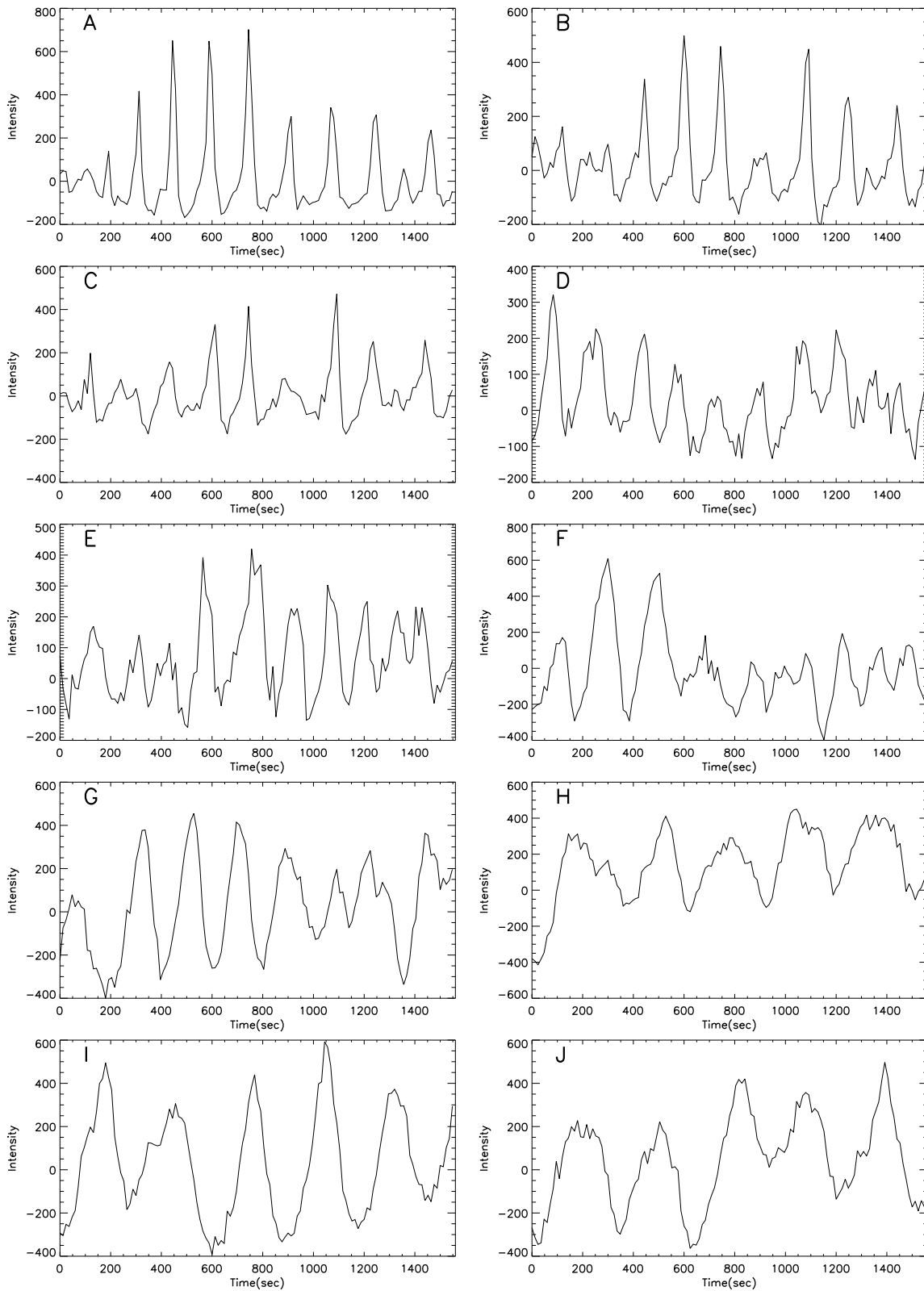


**Fig. 4** Time profiles of the  $H\alpha$  intensity variation (solid line) at the sample points A–J, respectively, in Fig. 1

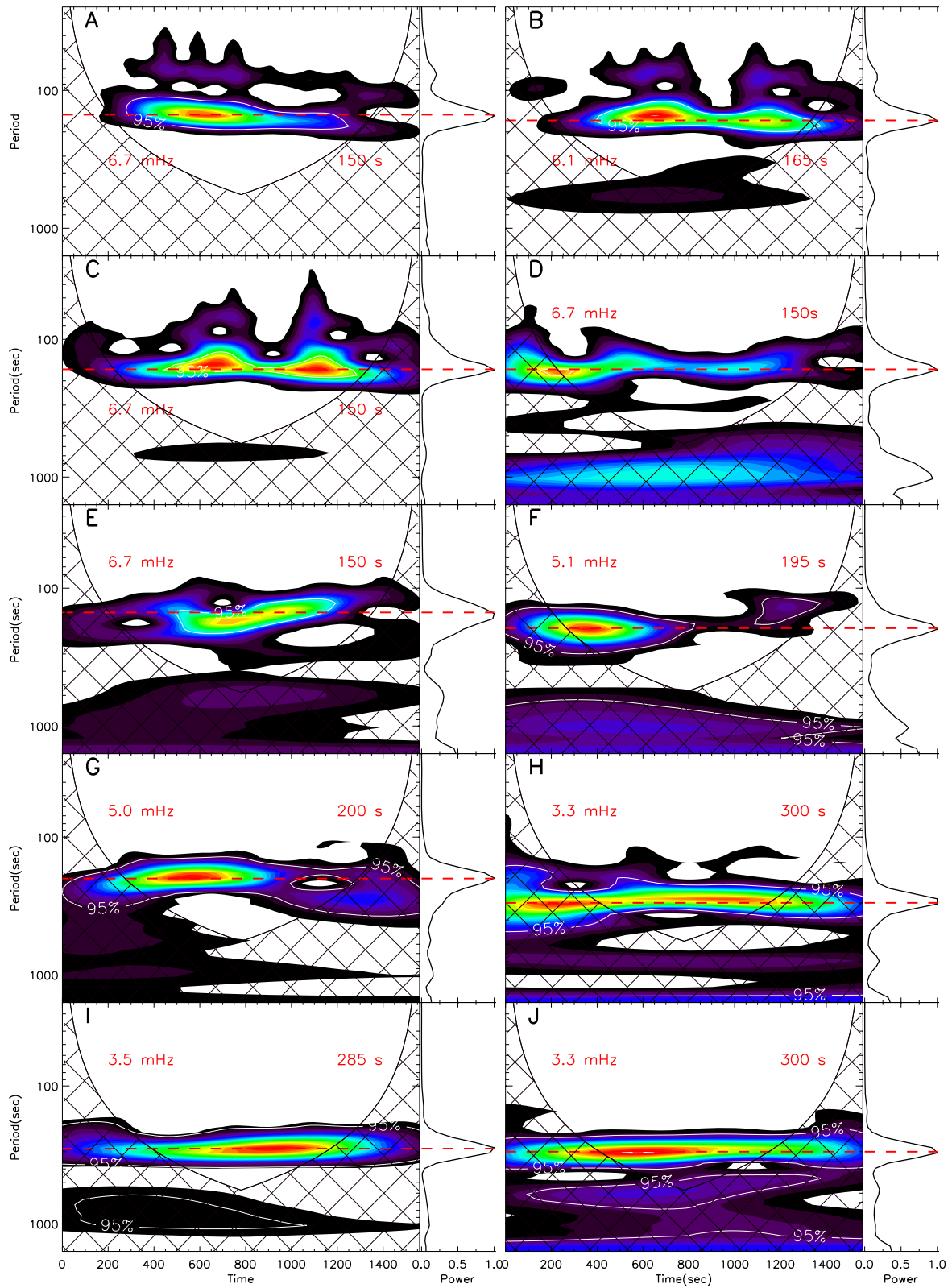
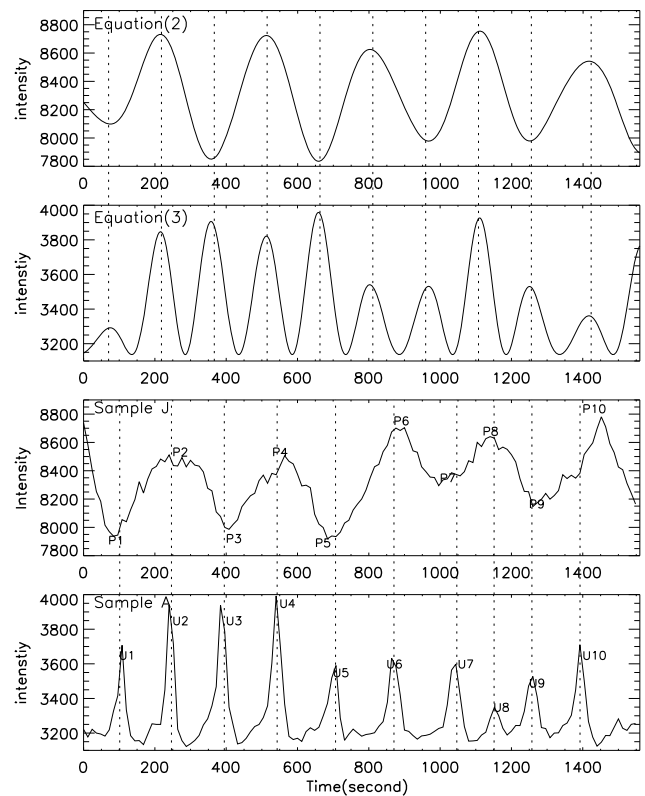


**Fig. 5** Wavelet analysis of the intensity variation curves of sample points (A–J). For each wavelet power spectrum, the corresponding normalized global power is plotted on the right. The red horizontal dashed

lines indicate the possible periods of the sample points, the significance level is above 95%. In this figure, redder color corresponds to the higher wavelet power. Taken from Zhou et al. (2017)

**Fig. 6** Simulated 5-min oscillation in the penumbra by using equation (2) (top panel), simulated 3-min oscillation in the umbra by using equation (3) (second panel). An  $H\alpha$  Doppler velocity variation of sample points J and A (third and fourth panels, respectively). Along one track of the running wave from source A to J, the oscillation of sample point J was delayed by about 396 s. The vertical dotted line shows the aligned 5-min and 3-min oscillations. Taken from Zhou et al. (2017)



5-min penumbra oscillations, and to understand the oscillation phenomena within sunspots. The oscillation sources with a period of 3-min are located in umbrae, while the oscillation sources with a period of 5-min are located around the umbra–penumbra boundary (Sych 2016).

In our analysis, it is found that the period of penumbral oscillations is twice that of the umbra oscillations. Furthermore, there is no smooth transition region from the former to the latter. When the background light intensity and the noise are filtered from the observations, the intensity profiles related to the oscillations can be expressed by the equation of a simple harmonic motion of the sample points:

$$X(x_n, y_n, t) = A(x_n, y_n, t) \cos(\omega t + \alpha) \tag{1}$$

where  $X$  is displacement,  $x_n$  and  $y_n$  are the coordinates of sample points,  $t$  is the time of oscillation,  $A$  is the amplitude, and  $\alpha$  is the initial phase. This oscillation causes the intensity periodicity change, and there may be a positive correlation between the intensity change and the amplitude  $X$  of running wave as shown in the following equation:

$$I_{osc}(x_n, y_n, t) = aA(x_n, y_n, t) \cos(\omega t + \alpha) + BL \quad (BL > 0). \tag{2}$$

On the other hand, when the sample points are in different medium the amplitude of the running waves may be propor-

tional to the square of the displacement  $X$ :

$$I_{osc}'(x_n', y_n', t') = bA^2(x_n', y_n', t') \cos^2(\omega t' + \alpha) + BL' \quad (BL' > 0). \tag{3}$$

The primed parameters in equation (3) represent the sample points in the medium which is different from that in equation (2),  $a$  and  $b$  are constant coefficients,  $BL$  is the background light intensity,  $I_{osc}$  is the observed oscillation intensity. We assumed that the oscillation in the umbra is represented by equation (3) and oscillation within penumbra is represented by equation (2). We used numerical simulation to plot the oscillation images of equations (2) and (3) in Fig. 5 (top and second panel). In order to confirm the theory, we plot the  $H\alpha$  intensity profiles at the sample points A and J independently. As shown in Fig. 4, the intensity variation of sample point J delays A by about 528 seconds. The markers U1–U10 and P1–P10 denote the wave crests or troughs of sample position A and J. The 5-min penumbral oscillation and 3-min umbral oscillation could be perfectly fitted by equations (2) and (3), respectively. Observing the vertical dotted line, we confirm that the period of 5-min penumbra is twice that of the 3-min umbral oscillation. Most of the peak values of sample point A could be matched to peak values and valley values of sample point J, although U10 and P10 have some deviation. At the same time, from equations (2) and (3) we can easily calculate the



period of 5-min and 3-min oscillations as  $\frac{2\pi}{\omega}$  and  $\frac{2\pi}{2\omega}$ , respectively. This suggests that the umbral and penumbral oscillations may be produced by a common physical mechanism. Power spectrum analysis in Fig. 5 shows that the oscillation frequencies in umbra and penumbra are about 6.55 and 3.37 mHz, respectively. Near the boundary, the frequency is 5.05 mHz. The steeply reducing frequency at the umbra–penumbra boundary cannot be easily explained. In Figs. 2 and 3, we can find that the running waves propagate from the wave source A in the umbra, run smoothly through the umbra–penumbra boundary, and then continuously propagate to the outer edge of the penumbra. However, the oscillation frequency in the sunspot has a steep drop at the umbra–penumbra boundary. The oscillation power may have a close relationship to the magnetic field strength and angle of inclination. Tziotziou et al. (2006) stated that the frequency jump should have close connection with the jump of inclination angles at the umbra–penumbra boundary. Maurya et al. (2013) showed that the oscillation frequency not only depends on the magnetic field inclination but also on the field strength. Ding et al. (2014) also confirmed that the short-period oscillations are commonly constrained within umbra, while long-period oscillations generally appear in the penumbra. They reconstructed the magnetic field inclination with the magneto-acoustic gravity wave theory and confirmed that the inclined magnetic field decreases the cut-off frequency. Löhner-Böttcher et al. (2015) retrieved the dominating wave periods and reconstructed the zenith inclinations in the chromosphere and upper photosphere; the results show that sunspot's magnetic field in the chromosphere inclines from almost vertical  $0^\circ$  in the umbra to around  $60^\circ$  in the outer penumbra. The penumbral magnetic field inclination decreases along with the increasing altitude. With the increasing altitude in the sunspot atmosphere, the magnetic field of the penumbra becomes less inclined. With the help of the Dopplergrams and magnetograms obtained by SOHO/MDI, Mathew (2008) revealed that the inclination of the magnetic field may enhance p-mode absorption near the umbra–penumbra boundary, where the inclination angle is nearly  $135^\circ$  (Mathew 2008; Gosain et al. 2011). By using the images obtained by both ground- and space-based telescopes, Jess et al. (2013) also found that the magnetic field inclination angles may play an important role in the propagation characteristics of the running penumbral waves.

As for the propagating velocity of the running waves which decreases along with the waves away from the umbra center, the explanation may be as follows: (i) the decrease is caused by changes of the physical properties when moving away from the umbra center, such as the plasma density, magnetic field strength, the magnetic field inclination; (ii) one has to recall the effect of the Evershed flow. As early as 1984, Zhugzhda and Dzhaliyov (1984) suggested

that the inverse Evershed flow may decrease the substantial frequency and radial phase speed of the running wave when the latter propagates from the umbra to the penumbra. Tsiropoula et al. (1996a, 1996b) and Georgakilas et al. (2003) proved that Evershed flow has radial inflow with velocities of about  $4 \text{ km s}^{-1}$  and  $6 \text{ km s}^{-1}$  at  $H\alpha \pm 0.3 \text{ \AA}$ , respectively. When the running waves propagate against the Evershed flow, the propagation velocity may decrease and the oscillation frequency may change.

More theoretical analysis and further observations are needed to exploit all possible scenarios. Further analysis is also needed for the clarification of the relation of the 3-min umbra and 5-min penumbra oscillations, this will be done based on a higher resolution telescope.

**Acknowledgements** This work is supported by the National Nature Science Foundation of China (11363007) and the Key laboratory of colleges and universities in Yunnan province for the high energy astrophysics. We would like to thank Zhi Xu, Zhong Liu, and the staff of the Fuxian Solar Observatory for their warm hospitality and help with the observations. Wavelet software was provided by C. Torrence and G. Compo, and is available at <http://paos.colorado.edu/research/wavelets>.

## References

- Alissandrakis, C.E., Georgakilas, A.A., Dialetis, D.: *Sol. Phys.* **138**, 93 (1992)
- Alissandrakis, C.E., Tsiropoula, G., Mein, P.: *Astron. Soc. Pac. Conf. Ser.* **115**, 49A (1998)
- Alissandrakis, C.E., Tsiropoula, G., Mein, P.: In: *ESA SP-448, Proceedings of 9th European Meeting on Solar Physics Magnetic Fields and Solar Processes* (Florence, Italy), p. 217A (1999)
- Beckers, J.M., Schultz, R.B.: *Sol. Phys.* **27**, 61 (1972)
- Beckers, J.M., Tallant, P.E.: *Sol. Phys.* **7**, 351 (1969)
- Bhatnagar, A., Livingston, W.C., Harvey, J.W.: *Sol. Phys.* **27**, 80 (1972)
- Bogdan, T.J., Judge, P.G.: *Philos. Trans. R. Soc. Lond. A* **364**, 313 (2006)
- Christopoulou, E.B., Georgakilas, A.A., Koutchmy, S.: *Astron. Astrophys.* **354**, 305 (2000)
- Christopoulou, E.B., Georgakilas, A.A., Koutchmy, S.: *Astron. Astrophys.* **375**, 616–628 (2001)
- Ding, Y., Sych, R., Reznikova, V.E., Nakariakov, V.M.: *Astrophys. J.* (2014). [arXiv:1211.5196v2](https://arxiv.org/abs/1211.5196v2)
- Evans, D.J., Roberts, B.: *Astrophys. J.* **348**, 346 (1990)
- Georgakilas, A.A., Christopoulou, E.B., et al.: *Astron. Astrophys.* **403**, 1123–1133 (2003)
- Giovanelli, R.G.: *Sol. Phys.* **27**, 71 (1972)
- Gosain, S., Mathew, S.K., Venkatakrishnan, P.: *Sol. Phys.* **268**, 335 (2011)
- Jess, D.B., Reznikova, V.E., et al.: *Astrophys. J.* **779**, 168J (2013)
- Kobanov, N.I., Makarchik, D.V.: *Astron. Astrophys.* **424**, 671–675 (2004)
- Liang, H.F., Yang, W.G., Ma, L., Yang, R.J.: *New Astron.* **17**, 112L (2012)
- Löhner-Böttcher, J., Bello González, N.: *Astron. Astrophys.* **580**, 53 (2015)
- Löhner-Böttcher, J., Bello González, N., Schmidt, W.: (2015). [arXiv:1601.05925](https://arxiv.org/abs/1601.05925)
- Mathew, S.K.: *Sol. Phys.* **251**, 515 (2008)

- Maurya, R.A., Chae, J., Park, H., Yang, H., Song, D., Cho, K.: *Sol. Phys.* **288**, 73–88 (2013)
- Roupe van der Voort, L.H.M., Rutten, J., Sütterlin, R.P., et al.: *Astron. Astrophys.* **403**, 277–285 (2003)
- Shen, Y.D., Liu, Y.: *Astrophys. J.* **754**, 7 (2012a)
- Shen, Y.D., Liu, Y.: *Astrophys. J.* **753**, 53 (2012b)
- Shen, Y.D., Liu, Y.: *Astrophys. J.* **752**, L23 (2012c)
- Shen, Y.D., Liu, Y., Su, J.T., et al.: *Sol. Phys.* **288**, 585 (2013b)
- Shen, Y.D., Liu, Y., Su, J.T., Li, H., Zhao, R.J.: *Astrophys. J.* **773**, L33 (2013a)
- Shen, Y.D., Ichimoto, K., Ishii, T.T., et al.: *Astrophys. J.* **786**, L51 (2014a)
- Shen, Y.D., Liu, Y.D., Chen, P.F., et al.: *Astrophys. J.* **795**, 130 (2014b)
- Shen, Y.D., Liu, Y., Liu, Y.D., et al.: *Astrophys. J.* **814**, 17 (2015)
- Su, J.T., Ji, K.F., Cao, W., et al.: *Astrophys. J.* **817**, 117 (2016)
- Sych, R.: In: AGU (Washington, DC), Geophysical Monograph Series, vol. 216, p. 467S (2016)
- Tsiropoula, G., Alissandrakis, C.E., Dialetis, D., Mein, P.: *Sol. Phys.* **167**, 79 (1996a)
- Tsiropoula, G., Alissandrakis, C.E., Dialetis, D., Mein, P.: *Sol. Phys.* **167**, 79T (1996b)
- Tsiropoula, G., Alissandrakis, C.E., Mein, P.: *Astron. Astrophys.* **355**, 375–380 (2000)
- Tziotziou, K., Tsiropoula, G., Mein, N., Mein, P.: *Astron. Astrophys.* **689**, 695 (2006)
- Zhou, X.P., Liang, H.F., Li, Q.H., et al.: *New Astron.* **51**, 86Z (2017)
- Zhugzhda, Y.D., Dzhaliyov, N.S.: *Astron. Astrophys.* **133**, 333–340 (1984)
- Zirin, H., Stein, A.: *Astrophys. J.* **178**, L85 (1972)